

Contents lists available at [ScienceDirect](http://ScienceDirect)

## Physics Letters B

[www.elsevier.com/locate/physletb](http://www.elsevier.com/locate/physletb)

## Probing bino–gluino coannihilation at the LHC

Natsumi Nagata<sup>a,b,\*</sup>, Hidetoshi Otono<sup>c</sup>, Satoshi Shirai<sup>d</sup><sup>a</sup> William I. Fine Theoretical Physics Institute, School of Physics and Astronomy, University of Minnesota, Minneapolis, MN 55455, USA<sup>b</sup> Kavli Institute for the Physics and Mathematics of the Universe (WPI), The University of Tokyo Institutes for Advanced Study, The University of Tokyo, Kashiwa 277-8583, Japan<sup>c</sup> Research Center for Advanced Particle Physics, Kyushu University, Fukuoka 812-8581, Japan<sup>d</sup> Deutsches Elektronen-Synchrotron (DESY), 22607 Hamburg, Germany

## ARTICLE INFO

## Article history:

Received 12 April 2015

Received in revised form 11 June 2015

Accepted 18 June 2015

Available online 19 June 2015

Editor: G.F. Giudice

## ABSTRACT

It has been widely known that bino-like dark matter in the supersymmetric (SUSY) theories in general suffers from over-production. The situation can be drastically improved if gluinos have a mass slightly heavier than the bino dark matter as they reduce the dark matter abundance through coannihilation. In this work, we consider such a bino–gluino coannihilation scenario in high-scale SUSY models, which can be actually realized when the squark-mass scale is less than 100–1000 TeV. We study the prospects for exploring this bino–gluino coannihilation scenario at the LHC. We show that the searches for long-lived colored particles with displaced vertices or large energy loss offer a strong tool to test this scenario in collider experiments.

© 2015 The Authors. Published by Elsevier B.V. This is an open access article under the CC BY license (<http://creativecommons.org/licenses/by/4.0/>). Funded by SCOAP<sup>3</sup>.

## 1. Introduction

The first stage of the LHC running has pointed a possible direction for the actual realization of the supersymmetric (SUSY) standard model (SM). First and foremost, the observed SM-like Higgs boson [1] with a mass of about 125 GeV [2] implies that the mass scale of SUSY particles is higher than the electroweak scale; the radiative corrections by stops easily lift up the Higgs mass from the tree-level value predicted to be less than the  $Z$ -boson mass in the minimal SUSY SM [3], if the stop masses are far above the electroweak scale [4,5]. This is in fact consistent with lack of any evidence in the SUSY searches so far [6,7]. A relatively high SUSY breaking scale offers further advantages for SUSY SMs. For instance, heavy masses of SUSY particles suppress the flavor changing neutral current processes as well as the electric dipole moments of the SM particles [8,9], which are stringently constrained by the low-energy precision experiments. Moreover, such heavy SUSY particles reduce the proton decay rate via the color-triplet Higgs exchange [10] and make the simplest version of the SUSY grand unification model [11] viable. In cosmology, the gravitino problem is evaded when the gravitino mass is high enough [12]. These attractive

points stimulate quite a few studies of high-scale SUSY models [13–21].

An order parameter of SUSY breaking is the gravitino mass  $m_{3/2}$ . If the SUSY breaking effects are transmitted to the visible sector via the gravitational interactions (or other interactions suppressed by some high-scale cutoff such as the Planck scale), then the soft SUSY-breaking scalar masses are induced with their size being  $\mathcal{O}(m_{3/2})$ . In this case, the scalar SUSY particles typically have masses of the order of  $m_{3/2}$ ; from now on, we express the typical masses of these scalar particles by  $\tilde{m} \sim m_{3/2}$ . The masses of the fermionic SUSY particles (gauginos and Higgsinos) are, on the other hand, dependent on models, since their mass terms can be suppressed if there exist additional symmetries. For example, the gaugino masses become much smaller than the gravitino mass if the SUSY breaking fields are charged under some symmetry. In this case, these masses are generated by quantum effects, such as anomaly mediation contribution [22,23] and threshold corrections at the SUSY breaking scale [22,24]. They are also affected by the presence of extra particles [25]. Moreover, the Higgsino mass can be suppressed by, e.g., the Peccei–Quinn symmetry [26] and be much lighter than  $m_{3/2}$  and  $\tilde{m}$ . See for instance Refs. [27,28] for a concrete realization of light Higgsinos.

Possible deviation of the masses of the fermionic SUSY partners from  $m_{3/2}$  and  $\tilde{m}$  gives additional benefits to SUSY SMs. Firstly, if gauginos lie around  $\mathcal{O}(1)$  TeV, gauge coupling unification is realized with great precision [29] even when the scalar mass scale  $\tilde{m}$  is much higher than the electroweak scale. Secondly, the neutral

\* Corresponding author at: William I. Fine Theoretical Physics Institute, School of Physics and Astronomy, University of Minnesota, Minneapolis, MN 55455, USA.

E-mail address: [natsumi.nagata@ipmu.jp](mailto:natsumi.nagata@ipmu.jp) (N. Nagata).

components of these fermions, the neutral bino, wino, and Higgsino, can be a candidate for dark matter (DM) in the Universe. Among them, the neutral wino is one of the most promising candidates since the anomaly mediation mechanism naturally makes the wino be the lightest SUSY particle (LSP). Its thermal relic abundance actually explains the observed DM density if the wino mass is around 3 TeV [30]. Currently the mass of the wino LSP  $M_{\tilde{W}}$  is restricted by the direct search at the LHC as  $M_{\tilde{W}} > 270$  GeV [31]. The wino DM scenario is also being constrained by the indirect DM searches using gamma rays [32,33]. These experiments, as well as the DM direct detection experiments [34], can probe this scenario in future. Higgsino DM with a mass of  $\sim 1$  TeV can also account for the observed DM density [35]. For the recent study of the phenomenology and future prospects for this Higgsino DM scenario, see Ref. [36] and references therein.

The last possibility is bino DM. If the scalar SUSY particles and Higgsino are significantly heavy, bino DM is usually over-produced as the interactions of bino with the SM sector tend to be suppressed. To avoid the over-production and get correct dark matter abundance, we need some exceptional mechanism to reduce the bino abundance, such as coannihilation and Higgs funnel [37]. If the Higgsino mass is heavier than  $\mathcal{O}(10)$  TeV, the remaining possibility is the coannihilation. In this case, its thermal relic agrees to the observed value if there exist some particles degenerate with the bino DM in mass. In fact, as shown in Refs. [38–43], bino DM can explain the correct DM density if wino or gluino has a mass slightly above the bino mass. After all, there are various options for DM candidates in the high-scale SUSY scenario, and therefore it is quite important to experimentally examine each possibility.

Among the possibilities mentioned above, the collider testability of the bino–gluino coannihilation is expected to be the most promising since this case requires light gluinos. As we shall see below, we expect an  $\mathcal{O}(1)$  TeV gluino mass in this case, which can be within the reach of the LHC. This could be compared to other DM scenarios in high-scale SUSY models; for instance, if the gaugino masses follow the spectrum predicted by the anomaly mediation, wino is the LSP and it becomes the main component of DM if it has a mass of 3 TeV, as mentioned above. In this case, the gluino mass is predicted to be  $\mathcal{O}(10)$  TeV, which is of course far above the possible reach of the LHC. In this sense, it could be much easier to look for gluinos in the bino–gluino scenario than other cases. This naive expectation, however, turns out to be questionable. The bino–gluino coannihilation scenario requires that the mass difference between bino and gluino,  $\Delta M$ , be  $\Delta M \lesssim 100$  GeV. Such small mass difference results in soft jet emissions, which make it extremely challenging to detect the signal of gluino production. For this reason, previous studies have concluded that it is difficult to probe this bino–gluino coannihilation scenario at the LHC if the DM mass is heavier than 1 TeV [42,44,45].

In this work, we show that this small mass difference actually helps us to probe the bino–gluino coannihilation. When  $\Delta M \lesssim 100$  GeV and the sfermion masses are much heavier than the gaugino masses, the lifetime of gluinos  $\tau_{\tilde{g}}$  can be long enough to distinguish its decay signal from that of prompt decay. As will be shown below, we expect its decay length to be  $c\tau_{\tilde{g}} \gtrsim \mathcal{O}(1)$  mm when the sfermion masses are  $\mathcal{O}(100)$  TeV. A decay length of this order is in fact the main target of searches for long-lived colored particles with displaced vertices (DVs) [46] and large energy loss [47]. We will find that this search technique indeed gives a stringent limit on the bino–gluino coannihilation region, and probe wide range of the parameter space in future experiments.

This paper is organized as follows. In the next section, we consider the bino–gluino coannihilation scenario and show the parameter region which accomplishes the correct DM density. The lifetime of gluino predicted in this parameter region is given in

Section 3. Then, in Section 4, we discuss the strategy of the long-lived gluino searches at the LHC, and present the current constraint and future prospects for the bino–gluino coannihilation scenario. Finally, Section 5 is devoted to conclusion and discussion.

## 2. Bino–gluino coannihilation

To begin with, let us discuss the bino–gluino coannihilation scenario [39–43] to clarify the target parameter space we consider in the following analysis. Throughout this paper, bino is assumed to be the LSP and be the DM in the Universe. We consider the case where the bino–gluino coannihilation is effective so that the thermal relic abundance of the bino LSP is consistent with the observed DM density  $\Omega_{\text{DM}} h^2 = 0.12$ . Thus, bino and gluino should be degenerate in mass, *i.e.*,  $\Delta M \equiv M_{\tilde{g}} - M_{\tilde{B}} \lesssim 100$  GeV, with  $M_{\tilde{g}}$  and  $M_{\tilde{B}}$  being the gluino and bino masses, respectively. We further assume that the typical mass of scalar SUSY particles,  $\tilde{m}$ , as well as the Higgsino mass  $M_{\tilde{H}}$ , is as high as the gravitino mass  $m_{3/2}$ . This setup is realized with a generic Kähler potential. The gaugino masses are supposed to be suppressed by a loop factor compared with  $m_{3/2}$ , which occurs when the SUSY breaking superfields are non-singlet. Namely, we require  $M_{\tilde{B}} \sim M_{\tilde{g}} \ll \tilde{m} \sim M_{\tilde{H}} \sim m_{3/2}$  in what follows. Moreover, we assume the wino is heavy enough not to contribute to the coannihilation process. It turns out that such a mass spectrum can be in fact realized in the high-scale SUSY models [25,42]. We will see below that the scalar mass scale  $\tilde{m}$  gives the significant effects on the determination of the bino DM abundance.<sup>1</sup>

The relevant annihilation processes to the computation of the thermal relic abundance are the self-annihilation and coannihilation of bino and gluinos. Among them, gluino self-annihilation is the most effective because of the strong interaction, and this plays the dominant role in the determination of the bino relic abundance. The bino self-annihilation and bino–gluino annihilation are much smaller than the gluino self-annihilation, since these cross sections are suppressed by heavy Higgsino and sfermion masses. Hence, these annihilation processes scarcely affect the following calculation.

An important caveat here is that the bino–gluino coannihilation does not work efficiently without chemical equilibrium between bino and gluinos [43,48]. Therefore we should require that the transition rate between them should be fast enough compared to the Hubble expansion rate. The transition rate is, however, again suppressed by heavy squark masses. Thus, we obtain an upper bound on  $\tilde{m}$  by imposing the above condition. The transition rate of bino into gluino via quark scattering,  $\Gamma(\tilde{B}q \rightarrow \tilde{g}q)$ , is estimated by the product of the corresponding scattering cross section,  $\sigma(\tilde{B}q \rightarrow \tilde{g}q)$ , and the number density of initial state quarks,  $n_q$ . The former is approximately given by  $\sigma(\tilde{B}q \rightarrow \tilde{g}q) \sim T^2/\tilde{m}^4$  with  $T$  being the temperature of the Universe, while the latter is  $n_q \sim T^3$  since quarks are relativistic when the transition process is active. Consequently, the transition rate is given by

$$\Gamma(\tilde{B}q \rightarrow \tilde{g}q) \sim \frac{T^5}{\tilde{m}^4}. \quad (1)$$

On the other hand, the Hubble rate  $H$  goes like  $H \sim T^2/M_{\text{Pl}}$  with  $M_{\text{Pl}}$  the Planck scale in the radiation dominated epoch. In order to sufficiently reduce the bino density through coannihilation, the condition  $\Gamma(\tilde{B}q \rightarrow \tilde{g}q) \gg H$  should be satisfied until the bino DM decouples from thermal bath at the freeze-out temperature  $T_f \sim M_{\tilde{B}}/20$ . This reads

<sup>1</sup> While completing this manuscript, we received Ref. [43], which also discusses the squark mass effects in the gluino coannihilation scenario.

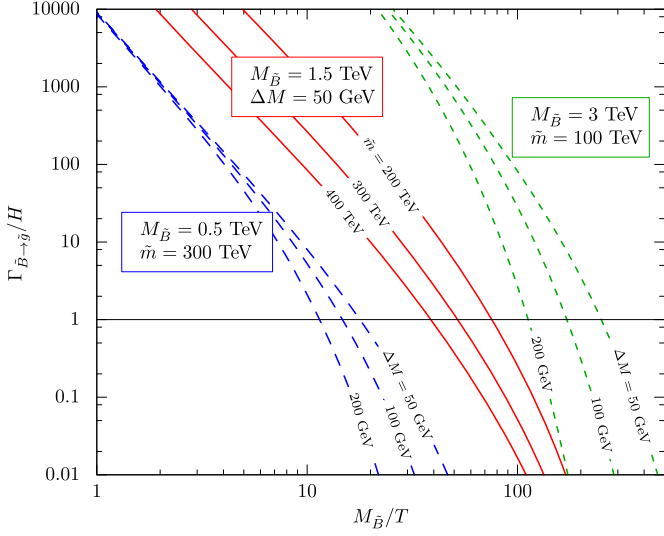


**Fig. 1.** Ratio of the bino–gluino conversion rate to the Hubble rate as functions of  $M_{\tilde{B}}/T$ . We set  $M_{\tilde{B}} = 1.5$  TeV,  $\Delta M = 50$  GeV and  $\tilde{m} = (200, 300, 400)$  TeV in the red solid lines;  $M_{\tilde{B}} = 0.5$  TeV,  $\tilde{m} = 300$  TeV and  $\Delta M = (50, 100, 200)$  GeV in blue and dashed lines and  $m_{\tilde{B}} = 3$  TeV,  $\tilde{m} = 100$  TeV and  $\Delta M = (50, 100, 200)$  GeV in green and dotted lines. (For interpretation of the references to color in this figure legend, the reader is referred to the web version of this article.)

$$\frac{\tilde{m}^4}{M_{\text{Pl}}} \lesssim \left( \frac{M_{\tilde{B}}}{x_f} \right)^3, \quad (2)$$

which then gives an upper bound on the scalar mass scale  $\tilde{m}$ . Here  $x_f \equiv M_{\tilde{B}}/T_f \sim 20$ . Numerically, we have

$$\tilde{m} \lesssim 250 \times \left( \frac{M_{\tilde{B}}}{1 \text{ TeV}} \right)^{\frac{3}{4}} \text{ TeV}. \quad (3)$$

We find that when the DM mass is  $\mathcal{O}(1)$  TeV the upper bound on the scalar mass scale lies around  $\mathcal{O}(10^{(2-3)})$  TeV; indeed, many high-scale SUSY models [13–21] predict the SUSY breaking scale to be this order, with which the 125 GeV Higgs mass is naturally accounted for. Therefore, it is quite important to take into account the constraint on  $\tilde{m}$  when we discuss the bino–gluino annihilation in the high-scale SUSY scenario.

To make the above discussion more accurately, we perform the numerical computation by solving the Boltzmann equation to obtain the bino–gluino conversion rate and the resultant relic abundance. First, in Fig. 1, we show the ratio of the bino–gluino conversion rate  $\Gamma_{\tilde{B} \to \tilde{g}}$  with respect to the Hubble rate  $H$  as functions of  $M_{\tilde{B}}/T$ . Here, we set  $M_{\tilde{B}} = 1.5$  TeV,  $\Delta M = 50$  GeV and  $\tilde{m} = (200, 300, 400)$  TeV in the red solid lines;  $M_{\tilde{B}} = 0.5$  TeV,  $\tilde{m} = 300$  TeV and  $\Delta M = (50, 100, 200)$  GeV in the blue dashed lines;  $M_{\tilde{B}} = 3$  TeV,  $\tilde{m} = 100$  TeV and  $\Delta M = (50, 100, 200)$  GeV in the green dotted lines. All of the squark masses are assumed to be equal to the universal mass  $\tilde{m}$ . When we evaluate the transition cross sections and (inverse) decay rate of gluino and bino, we use the effective theoretical approach to properly deal with sizable quantum corrections resulting from large difference between the gluino and squark mass scales; we first integrate out squarks to obtain a set of dimension-six operators which involve quarks, bino and gluino, and then evolve these operators down to the gluino mass scale by using the renormalization group equations, which results in a several tens percent enhancement of the transition rate, compared to the tree level calculation [49–51]. The loop-induced dimension-five dipole operator (gluon–bino–gluino) is found to be quite suppressed and thus its contribution is negligible in the present analysis. In addition, we include the so-called Sommerfeld effects [52] on the

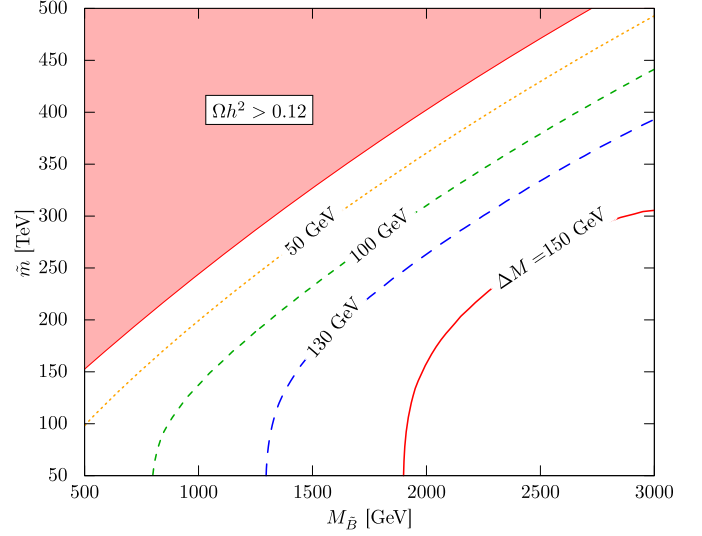


**Fig. 2.** Contour for the mass difference  $\Delta M$  which makes the thermal relic abundance of bino DM equal to the observed DM density  $\Omega_{\text{DM}} h^2 = 0.12$ . In the red shaded region the bino DM is overproduced due to failure of bino–gluino coannihilation. (For interpretation of the references to color in this figure legend, the reader is referred to the web version of this article.)

gluino annihilation. On top of that,  $p$ -wave contribution, finite-temperature effects, the scale dependence of the strong coupling constant in the QCD potential [41], possible ambiguity in the initial state color arrangement<sup>2</sup> due to thermal effects [53], and the bound-state effects on a pair of gluinos [43] may change the results by a factor of  $\mathcal{O}(10)\%$ . The above figure shows that the conversion rate decreases as  $\tilde{m}$  or  $\Delta M$  is taken to be larger. In particular, if the squark mass scale  $\tilde{m}$  is several hundred of TeV with the DM mass being a relatively small, then the condition  $\Gamma_{\tilde{B} \to \tilde{g}} \gg H$  does not hold any more when the DM abundance freezes out.

In Fig. 2, we plot on the  $M_{\tilde{B}} - \tilde{m}$  plane the mass difference  $\Delta M$  with which the thermal relic abundance of bino DM explains the observed DM density  $\Omega_{\text{DM}} h^2 = 0.12$ . In the red shaded region, the squark mass is too heavy for the coannihilation process to work well and therefore the DM is overproduced. We will discuss how to probe the parameter space shown in Fig. 2 at the LHC in the subsequent section.

### 3. Gluino lifetime

Next, we study the lifetime of gluino, which plays a crucial role in the discussion of the testability of the bino–gluino coannihilation scenario at the LHC in the following section. As mentioned in the Introduction, in this scenario, a relatively light gluino mass is expected. Thus, the gluino pair production is suitable target for the hadron collider experiments like the LHC in this case. After the pair production, a gluino decays into a bino, a quark, and an anti-quark through the squark-exchange processes [49–51,54]. When the gluino is degenerate with the bino in mass, which is required in the bino–gluino coannihilation scenario, the decay length of the gluino,  $c\tau_{\tilde{g}}$ , is approximately given as follows:

$$c\tau_{\tilde{g}} = \mathcal{O}(1) \times \left( \frac{\Delta M}{100 \text{ GeV}} \right)^{-5} \left( \frac{\tilde{m}}{100 \text{ TeV}} \right)^4 \text{ cm}. \quad (4)$$

<sup>2</sup> In our computation, we assume that the initial state gluinos have a definite color configuration, not thermal averaged one.

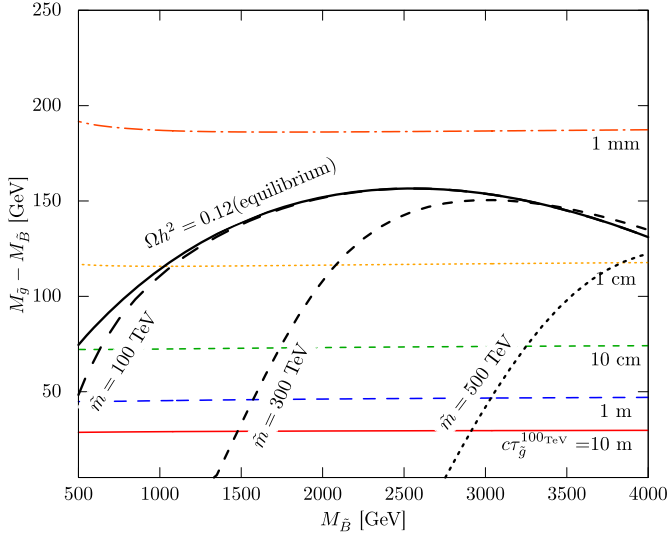


**Fig. 3.** Decay length of the gluino  $c\tau_{\tilde{g}}^{100\text{TeV}}$  with the squark mass  $\tilde{m} = 100$  TeV in colored (almost horizontal) lines. Mass difference  $\Delta M$  with which the thermal relic of the bino DM agrees to  $\Omega_{\text{DM}} h^2 = 0.12$  is also shown in the black solid line for the case in which the bino–gluino chemical equilibrium is assumed, while the cases for  $\tilde{m} = 100, 300$  and  $500$  TeV are given in the other black lines. (For interpretation of the references to color in this figure legend, the reader is referred to the web version of this article.)

From this equation, we see that the decay length gets longer as the mass difference  $\Delta M$  is taken to be smaller or the scalar mass scale  $\tilde{m}$  is set to be larger. Therefore, we expect a relatively long decay length when the bino–gluino coannihilation is achieved in the high-scale SUSY scenario.

To illustrate the gluino decay length corresponding to the bino–gluino coannihilation region, in Fig. 3, we plot contours of the gluino decay length in colored lines with the squark masses set to be  $\tilde{m} = 100$  TeV, which we denote by  $c\tau_{\tilde{g}}^{100\text{TeV}}$ , on the  $M_{\tilde{B}} - \Delta M$  plane. We also show the mass difference  $\Delta M$  with which the thermal relic of the bino DM agrees to  $\Omega_{\text{DM}} h^2 = 0.12$ ; the black solid line shows the case where the bino–gluino chemical equilibrium is assumed, while the other black lines represent the cases of  $\tilde{m} = 100, 300$  and  $500$  TeV. To avoid overproduction,  $\Delta M$  should be below these lines. From Fig. 3, we find that the gluino decay length is scarcely dependent on the bino mass, which has been already shown in Eq. (4) implicitly. We have  $c\tau_{\tilde{g}} > \mathcal{O}(1)$  mm where the thermal relic abundance of the bino DM explains the observed DM density. This is a crucial observation for the strategy of exploring the bino–gluino coannihilation region at the LHC.

#### 4. LHC search

If gluino decays promptly and the bino and gluino masses are almost degenerate, it is quite hard to search for the gluino at the LHC, since the small mass difference makes the missing energy and jet activities tiny. Currently the ATLAS and CMS Collaborations have put limits on such a degenerate neutralino, *i.e.*, bino in our case, with a mass of around 600 GeV [6,7]. The bounds are expected to reach  $\sim 1200$  GeV with the integrated luminosity of  $300 \text{ fb}^{-1}$  at the 14 TeV LHC [55].

These limits are in fact drastically improved once we consider the fact that in the case of the bino–gluino coannihilation scenario, the gluino lifetime is as long as  $c\tau_{\tilde{g}} > \mathcal{O}(1)$  mm, as we have seen in the previous section. Such a gluino has a distinct property in the collider experiments; a gluino with a decay length of  $c\tau_{\tilde{g}} > \mathcal{O}(1)$  mm leaves a visible displaced vertex (DV) in the detectors,

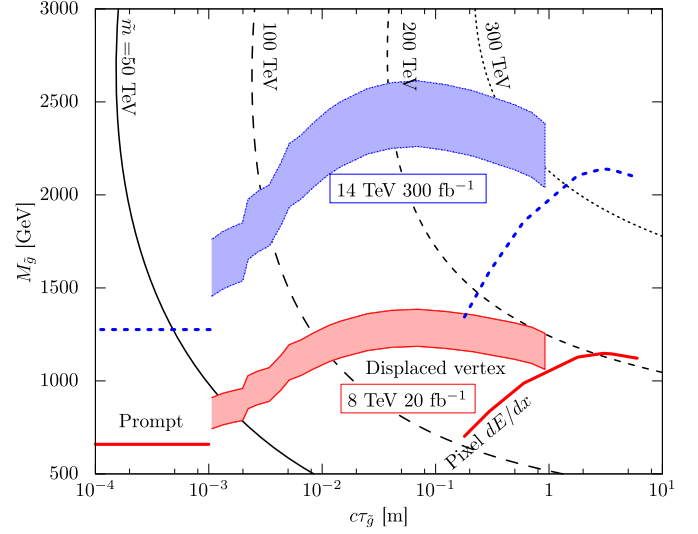


**Fig. 4.** Current constraints (red and solid lines) and future prospects (blue and dashed lines) for the gluino searches. Favored region for the DM relic abundance is also shown in black lines for the cases of  $\tilde{m} = 50, 100, 200,$  and  $300$  TeV, with  $\Delta M$  chosen so that the thermal relic abundance of the bino equals to the current observed DM density. We also show the current constraint [6] and future prospect of the 14 TeV LHC run [55] from the search for the prompt-decay gluino in horizontal red solid and blue dashed lines, respectively. (For interpretation of the references to color in this figure legend, the reader is referred to the web version of this article.)

which greatly helps the gluino search. At present, however, there have been no dedicated searches from this aspect so far.<sup>3</sup>

The ATLAS Collaboration has searched for DVs in the region of  $|z| < 30$  cm and  $r < 30$  cm in the inner detector [46,58,59], where  $z$ -axis points along the LHC beam line and  $r$  denotes the radial coordinate in the plane perpendicular to the  $z$ -axis. They use the DVs reconstructed only in the air-gap region, namely, discard the DVs reconstructed within the material layers. This leads to significant background reduction. The signal region for the DVs is defined such that the number of tracks associated with the DV is larger than four and  $m_{\text{DV}} > 10$  GeV, where  $m_{\text{DV}}$  is the invariant mass of the tracks evaluated with the charged-pion mass hypothesis. Since they have observed no event in the signal region, they have given an upper limit on the long-lived gluino production cross section, which is interpreted as bound on the gluino mass in the high-scale SUSY scenario with a fixed neutralino mass of 100 GeV [46].

We re-interpret this low  $m_{\text{DV}}$  search result in the case of the degenerate bino–gluino system, and obtain constraints on the bino–gluino coannihilation scenario, which is shown in Fig. 4. Here, the red and blue bands (from  $c\tau_{\tilde{g}} = 1$  mm to 1 m) show the estimated sensitivities of the DV search with the total luminosity of  $20 \text{ fb}^{-1}$  at the 8 TeV running and with  $300 \text{ fb}^{-1}$  at 14 TeV, respectively. The upper lines of these bands are for the cases where only the trigger efficiency is taken into account, which are simulated with HERWIG 6 [60] and ACERDET [61] to be 40% for 8 TeV with the threshold of the missing energy of 100 GeV, and 15% for 14 TeV with the missing energy trigger of 200 GeV. Their dependence on the mass of gluino is only a few percent level. The lower lines, on the other hand, correspond to the reconstruct-

<sup>3</sup> A similar discussion has been recently given in Ref. [56] based on the CMS displaced dijets results [57], though their constraint is much weaker than ours. As we will discuss below, the ATLAS DV search [46] exploits the missing energy trigger, while the CMS search does not. In addition, the CMS dijet search requires large scalar sum of jet transverse momenta, which is not effective when the mass difference of bino and gluino is small. For these reasons, at present, the ATLAS search offers better sensitivities than the CMS one.

tion efficiency for DVs that is estimated from Refs. [58], where the long-lived neutralino decaying to two quarks and one muon is discussed in the  $R$ -parity violating SUSY scenario. The reconstruction efficiency for the 108 GeV neutralino is about 20% of that for the 494 GeV neutralino in this case; we use this 20% for the lower lines, which gives conservative limits rather than the previous ones. In Fig. 4, we also show the favored region in terms of the DM relic abundance in black lines for the cases of  $\tilde{m} = 50, 100, 200,$  and  $300$  TeV. Here, the bino–gluino mass difference  $\Delta M$  is taken such that the thermal relic of bino DM explains the correct DM density. This reads that the present LHC data have already constrained a considerable range of parameter region consistent with the bino–gluino coannihilation scenario. This constraint is in fact much stronger than the ordinary limit from the searches of promptly decaying gluinos, which are based on only jets and missing energy [6,7]. This constraint is indicated by the red and solid horizontal line in this figure. The 14 TeV LHC running can further probe this scenario and reach  $M_{\tilde{g}} \sim 2.5$  TeV when  $c\tau_{\tilde{g}} = \mathcal{O}(1 - 10)$  cm; this sensitivity is better than that by search with only jets and missing energy [55] (shown in the horizontal blue dashed line in the above figure) by almost a factor of two.

In addition, the ATLAS Collaboration searches for massive charged meta-stable particles, such as  $R$ -hadrons [62], with an another approach [47]. A characteristic feature of such particles is that they are produced with relatively low velocities,  $\beta \equiv v/c < 1$ . This signature can be seen by means of large energy loss,  $dE/dx$ , in the ATLAS Pixel detector. Here, we note that this analysis requires gluinos to form charged  $R$ -hadrons. Although the estimation of the charged hadronization fraction of gluinos may suffer from large theoretical uncertainty, this search offers the best sensitivity for  $c\tau_{\tilde{g}} > 1$  m. In Ref. [47], the result of this search is given as limits on the gluino mass in the case of  $\Delta M = 100$  GeV. We use the trigger efficiency given there for our computation for the 8 TeV case, and estimate the efficiency for the 14 TeV case by re-scaling it with a factor obtained by simulations. The red and blue solid curves in Fig. 4 show the estimated sensitivities of this search with  $20 \text{ fb}^{-1}$  at 8 TeV and with  $300 \text{ fb}^{-1}$  at 14 TeV, respectively. We find that the searches of heavy stable charged particles give the most stringent constraints when  $c\tau_{\tilde{g}} > 1$  m, and are complementary to the DV searches. In particular, they are of importance when the scalar mass scale is relatively higher, say, a few hundred TeV.

## 5. Conclusion and discussion

In this paper, we study the bino–gluino coannihilation in the high-scale SUSY scenario. We have found that the squark mass scale cannot be too large for the coannihilation to work well. The upper bound on the squark mass is 200–1000 TeV for the gluino mass 1–8 TeV. Actually this mass scale is coincident with the prediction of the spectrum often called the spread or mini-split SUSY [13–21]. This constraint will provide a new perspective on the model-building to realize such mass spectrum.

We also discuss the LHC signatures of this scenario. Because of the small mass difference between the bino LSP and gluino, which is necessary for coannihilation, as well as heavy squark masses, the gluino decay length is considerably prolonged. Despite the small jets and missing energy activity, the DV and  $R$ -hadron searches can efficiently probe such long-lived gluinos. If the squark mass scale is higher than about 100 TeV, the current lower bound on the gluino mass is around 1.2 TeV. The 13/14 TeV LHC  $300 \text{ fb}^{-1}$  stage is expected to be able to explore gluinos with a mass of  $\sim 2$  TeV.

Let us speculate possible sensitivities for much higher energy machines. For gluinos with the decay length longer than  $\mathcal{O}(1)$  mm, a mass of 4.5 (10) TeV can be probed using an  $\sqrt{s} = 33$  (100) TeV running proton collider with the integrated luminosity of  $100 \text{ fb}^{-1}$ ,

provided that the background is sufficiently small and the detection efficiency of gluinos is the same as that of the current LHC detector. This estimation may, of course, be too naive. Further detailed studies should be dedicated to see more precise prospects for such colliders, though we expect that they can probe the most of parameter space of the bino–gluino coannihilation.

Lastly, we discuss the possibility of other gaugino coannihilation scenarios. As in the case of the current study, the small mass difference and heavier sfermion scale easily make the next LSP live long. For instance, in the case of the wino and gluino coannihilation, we may observe very exotic signatures; if the gluino lifetime is long enough, the gluino can carry the charged wino to the LHC trackers. In this case, we may observe displaced and disappearing tracks of the charged wino. The large gluino production cross section and the long-lived nature of the charged wino make it rather easy to look for this scenario in the LHC experiments. Another very interesting and plausible possibility is bino–wino coannihilation. This spectrum can be relatively easily realized even in the minimal anomaly mediation model. In this case, we may have another long-lived particle, which may play an important role at the LHC searches. A detailed analysis for this scenario will be done elsewhere [63].

## Acknowledgements

N.N. thanks Jason L. Evans and Keith A. Olive for useful discussions. The work of N.N. is supported by Research Fellowships of the Japan Society for the Promotion of Science for Young Scientists No. 26 · 8296.

## References

- [1] G. Aad, et al., ATLAS Collaboration, *Phys. Lett. B* 716 (2012) 1, arXiv:1207.7214 [hep-ex]; S. Chatrchyan, et al., CMS Collaboration, *Phys. Lett. B* 716 (2012) 30, arXiv:1207.7235 [hep-ex].
- [2] G. Aad, et al., ATLAS Collaboration, CMS Collaboration, *Phys. Rev. Lett.* 114 (2015) 191803, arXiv:1503.07589 [hep-ex].
- [3] K. Inoue, A. Kakuto, H. Komatsu, S. Takeshita, *Prog. Theor. Phys.* 67 (1982) 1889; R.A. Flores, M. Sher, *Ann. Phys.* 148 (1983) 95.
- [4] Y. Okada, M. Yamaguchi, T. Yanagida, *Prog. Theor. Phys.* 85 (1991) 1; Y. Okada, M. Yamaguchi, T. Yanagida, *Phys. Lett. B* 262 (1991) 54; J.R. Ellis, G. Ridolfi, F. Zwirner, *Phys. Lett. B* 257 (1991) 83; H.E. Haber, R. Hempfling, *Phys. Rev. Lett.* 66 (1991) 1815; J.R. Ellis, G. Ridolfi, F. Zwirner, *Phys. Lett. B* 262 (1991) 477.
- [5] G.F. Giudice, A. Strumia, *Nucl. Phys. B* 858 (2012) 63, arXiv:1108.6077 [hep-ph].
- [6] G. Aad, et al., ATLAS Collaboration, *J. High Energy Phys.* 1409 (2014) 176, arXiv:1405.7875 [hep-ex].
- [7] S. Chatrchyan, et al., CMS Collaboration, *J. High Energy Phys.* 1406 (2014) 055, arXiv:1402.4770 [hep-ex].
- [8] F. Gabbiani, E. Gabrielli, A. Masiero, L. Silvestrini, *Nucl. Phys. B* 477 (1996) 321, arXiv:hep-ph/9604387.
- [9] T. Moroi, M. Nagai, *Phys. Lett. B* 723 (2013) 107, arXiv:1303.0668 [hep-ph]; D. McKeen, M. Pospelov, A. Ritz, *Phys. Rev. D* 87 (2013) 113002, arXiv:1303.1172 [hep-ph]; W. Altmannshofer, R. Harnik, J. Zupan, *J. High Energy Phys.* 1311 (2013) 202, arXiv:1308.3653 [hep-ph]; K. Fuyuto, J. Hisano, N. Nagata, K. Tsumura, *J. High Energy Phys.* 1312 (2013) 010, arXiv:1308.6493 [hep-ph]; M. Tanimoto, K. Yamamoto, *Phys. Lett. B* 735 (2014) 426, arXiv:1404.0520 [hep-ph]; M. Tanimoto, K. Yamamoto, *Prog. Theor. Exp. Phys.* 053B07 (2015), arXiv:1503.06270 [hep-ph].
- [10] M. Liu, P. Nath, *Phys. Rev. D* 87 (2013) 095012, arXiv:1303.7472 [hep-ph]; J. Hisano, D. Kobayashi, T. Kuwahara, N. Nagata, *J. High Energy Phys.* 1307 (2013) 038, arXiv:1304.3651 [hep-ph]; M. Dine, P. Draper, W. Shepherd, *J. High Energy Phys.* 1402 (2014) 027, arXiv:1308.0274 [hep-ph]; N. Nagata, S. Shirai, *J. High Energy Phys.* 1403 (2014) 049, arXiv:1312.7854 [hep-ph]; L.J. Hall, Y. Nomura, S. Shirai, *J. High Energy Phys.* 1406 (2014) 137, arXiv:1403.8138 [hep-ph];

- J.L. Evans, N. Nagata, K.A. Olive, Phys. Rev. D 91 (2015) 055027, arXiv:1502.00034 [hep-ph].
- [11] N. Sakai, Z. Phys. C 11 (1981) 153;  
S. Dimopoulos, H. Georgi, Nucl. Phys. B 193 (1981) 150.
- [12] M. Kawasaki, K. Kohri, T. Moroi, A. Yotsuyanagi, Phys. Rev. D 78 (2008) 065011, arXiv:0804.3745 [hep-ph].
- [13] J.D. Wells, arXiv:hep-ph/0306127, 2003;  
J.D. Wells, Phys. Rev. D 71 (2005) 015013, arXiv:hep-ph/0411041.
- [14] N. Arkani-Hamed, S. Dimopoulos, J. High Energy Phys. 0506 (2005) 073, arXiv:hep-th/0405159;  
G. Giudice, A. Romanino, Nucl. Phys. B 699 (2004) 65, arXiv:hep-ph/0406088;  
N. Arkani-Hamed, S. Dimopoulos, G. Giudice, A. Romanino, Nucl. Phys. B 709 (2005) 3, arXiv:hep-ph/0409232;  
N. Arkani-Hamed, S. Dimopoulos, S. Kachru, arXiv:hep-th/0501082, 2005.
- [15] L.J. Hall, Y. Nomura, J. High Energy Phys. 1201 (2012) 082, arXiv:1111.4519 [hep-ph].
- [16] L.J. Hall, Y. Nomura, S. Shirai, J. High Energy Phys. 1301 (2013) 036, arXiv:1210.2395 [hep-ph].
- [17] M. Ibe, T. Moroi, T. Yanagida, Phys. Lett. B 644 (2007) 355, arXiv:hep-ph/0610277;  
M. Ibe, T.T. Yanagida, Phys. Lett. B 709 (2012) 374, arXiv:1112.2462 [hep-ph];  
M. Ibe, S. Matsumoto, T.T. Yanagida, Phys. Rev. D 85 (2012) 095011, arXiv:1202.2253 [hep-ph].
- [18] A. Arvanitaki, N. Craig, S. Dimopoulos, G. Villadoro, J. High Energy Phys. 1302 (2013) 126, arXiv:1210.0555 [hep-ph].
- [19] N. Arkani-Hamed, A. Gupta, D.E. Kaplan, N. Weiner, T. Zorawski, arXiv:1212.6971 [hep-ph], 2012.
- [20] J.L. Evans, M. Ibe, K.A. Olive, T.T. Yanagida, Eur. Phys. J. C 73 (2013) 2468, arXiv:1302.5346 [hep-ph];  
J.L. Evans, K.A. Olive, M. Ibe, T.T. Yanagida, Eur. Phys. J. C 73 (2013) 2611, arXiv:1305.7461 [hep-ph];  
J.L. Evans, M. Ibe, K.A. Olive, T.T. Yanagida, Eur. Phys. J. C 74 (2014) 2775, arXiv:1312.1984 [hep-ph];  
J.L. Evans, M. Ibe, K.A. Olive, T.T. Yanagida, Eur. Phys. J. C 74 (2014) 2931, arXiv:1402.5989 [hep-ph].
- [21] Y. Nomura, S. Shirai, Phys. Rev. Lett. 113 (2014) 111801, arXiv:1407.3785 [hep-ph].
- [22] G.F. Giudice, M.A. Luty, H. Murayama, R. Rattazzi, J. High Energy Phys. 9812 (1998) 027, arXiv:hep-ph/9810442.
- [23] L. Randall, R. Sundrum, Nucl. Phys. B 557 (1999) 79, arXiv:hep-th/9810155.
- [24] D.M. Pierce, J.A. Bagger, K.T. Matchev, R.-j. Zhang, Nucl. Phys. B 491 (1997) 3, arXiv:hep-ph/9606211.
- [25] A. Pomarol, R. Rattazzi, J. High Energy Phys. 9905 (1999) 013, arXiv:hep-ph/9903448;  
A.E. Nelson, N.J. Weiner, arXiv:hep-ph/0210288, 2002;  
K. Hsieh, M.A. Luty, J. High Energy Phys. 0706 (2007) 062, arXiv:hep-ph/0604256;  
A. Gupta, D.E. Kaplan, T. Zorawski, J. High Energy Phys. 1311 (2013) 149, arXiv:1212.6969 [hep-ph];  
K. Nakayama, T.T. Yanagida, Phys. Lett. B 722 (2013) 107, arXiv:1302.3332 [hep-ph];  
K. Harigaya, M. Ibe, T.T. Yanagida, J. High Energy Phys. 1312 (2013) 016, arXiv:1310.0643 [hep-ph];  
J.L. Evans, K.A. Olive, Phys. Rev. D 90 (2014) 115020, arXiv:1408.5102 [hep-ph].
- [26] R. Peccei, H.R. Quinn, Phys. Rev. Lett. 38 (1977) 1440.
- [27] K.J. Bae, H. Baer, H. Serce, Phys. Rev. D 91 (2015) 015003, arXiv:1410.7500 [hep-ph].
- [28] J.L. Evans, M. Ibe, K.A. Olive, T.T. Yanagida, Phys. Rev. D 91 (2015) 055008, arXiv:1412.3403 [hep-ph].
- [29] J. Hisano, T. Kuwahara, N. Nagata, Phys. Lett. B 723 (2013) 324, arXiv:1304.0343 [hep-ph].
- [30] J. Hisano, S. Matsumoto, M. Nagai, O. Saito, M. Senami, Phys. Lett. B 646 (2007) 34, arXiv:hep-ph/0610249.
- [31] G. Aad, et al., ATLAS Collaboration, Phys. Rev. D 88 (2013) 112006, arXiv:1310.3675 [hep-ex].
- [32] T. Cohen, M. Lisanti, A. Pierce, T.R. Slatyer, J. Cosmol. Astropart. Phys. 1310 (2013) 061, arXiv:1307.4082;  
J. Fan, M. Reece, J. High Energy Phys. 1310 (2013) 124, arXiv:1307.4400 [hep-ph];  
A. Hryczuk, I. Cholis, R. Iengo, M. Tavakoli, P. Ullio, J. Cosmol. Astropart. Phys. 1407 (2014) 031, arXiv:1401.6212 [astro-ph.HE].
- [33] B. Bhattacharjee, M. Ibe, K. Ichikawa, S. Matsumoto, K. Nishiyama, J. High Energy Phys. 1407 (2014) 080, arXiv:1405.4914 [hep-ph].
- [34] J. Hisano, K. Ishiwata, N. Nagata, Phys. Lett. B 690 (2010) 311, arXiv:1004.4090 [hep-ph];  
J. Hisano, K. Ishiwata, N. Nagata, Phys. Rev. D 82 (2010) 115007, arXiv:1007.2601 [hep-ph];  
J. Hisano, K. Ishiwata, N. Nagata, T. Takesako, J. High Energy Phys. 1107 (2011) 005, arXiv:1104.0228 [hep-ph];  
J. Hisano, K. Ishiwata, N. Nagata, Phys. Rev. D 87 (2013) 035020, arXiv:1210.5985 [hep-ph];  
J. Hisano, K. Ishiwata, N. Nagata, arXiv:1504.00915 [hep-ph], 2015.
- [35] M. Cirelli, A. Strumia, M. Tamburini, Nucl. Phys. B 787 (2007) 152, arXiv:0706.4071 [hep-ph].
- [36] N. Nagata, S. Shirai, J. High Energy Phys. 1501 (2015) 029, arXiv:1410.4549 [hep-ph].
- [37] K. Griest, D. Seckel, Phys. Rev. D 43 (1991) 3191.
- [38] H. Baer, T. Krupovnickas, A. Mustafayev, E.-K. Park, S. Profumo, et al., J. High Energy Phys. 0512 (2005) 011, arXiv:hep-ph/0511034.
- [39] S. Profumo, C. Yaguna, Phys. Rev. D 69 (2004) 115009, arXiv:hep-ph/0402208.
- [40] D. Feldman, Z. Liu, P. Nath, Phys. Rev. D 80 (2009) 015007, arXiv:0905.1148 [hep-ph].
- [41] A. De Simone, G.F. Giudice, A. Strumia, J. High Energy Phys. 1406 (2014) 081, arXiv:1402.6287 [hep-ph].
- [42] K. Harigaya, K. Kaneta, S. Matsumoto, Phys. Rev. D 89 (2014) 115021, arXiv:1403.0715 [hep-ph].
- [43] J. Ellis, F. Luo, K.A. Olive, arXiv:1503.07142 [hep-ph], 2015.
- [44] B. Bhattacharjee, A. Choudhury, K. Ghosh, S. Poddar, Phys. Rev. D 89 (2014) 037702, arXiv:1308.1526 [hep-ph].
- [45] M. Low, L.-T. Wang, J. High Energy Phys. 1408 (2014) 161, arXiv:1404.0682 [hep-ph].
- [46] G. Aad, et al., ATLAS Collaboration, arXiv:1504.05162 [hep-ex], 2015.
- [47] Search for metastable heavy charged particles with large ionisation energy loss in pp collisions at  $\sqrt{s} = 8$  TeV using the ATLAS experiment, Tech. Rep. ATLAS-CONF-2015-013, 2015.
- [48] G.R. Farrar, E.W. Kolb, Phys. Rev. D 53 (1996) 2990, arXiv:astro-ph/9504081;  
D.J. Chung, G.R. Farrar, E.W. Kolb, Phys. Rev. D 56 (1997) 6096, arXiv:astro-ph/9703145.
- [49] P. Gambino, G. Giudice, P. Slavich, Nucl. Phys. B 726 (2005) 35, arXiv:hep-ph/0506214.
- [50] R. Sato, S. Shirai, K. Tobioka, J. High Energy Phys. 1211 (2012) 041, arXiv:1207.3608 [hep-ph].
- [51] R. Sato, S. Shirai, K. Tobioka, J. High Energy Phys. 1310 (2013) 157, arXiv:1307.7144 [hep-ph].
- [52] J. Hisano, S. Matsumoto, M.M. Nojiri, Phys. Rev. Lett. 92 (2004) 031303, arXiv:hep-ph/0307216;  
J. Hisano, S. Matsumoto, M.M. Nojiri, O. Saito, Phys. Rev. D 71 (2005) 063528, arXiv:hep-ph/0412403.
- [53] A. Ibarra, A. Pierce, N. Shah, S. Vogl, Phys. Rev. D 91 (2015) 095018, arXiv:1501.03164 [hep-ph].
- [54] M. Toharia, J.D. Wells, J. High Energy Phys. 0602 (2006) 015, arXiv:hep-ph/0503175.
- [55] The ATLAS Collaboration, ATL-PHYS-PUB-2014-010, 2014.
- [56] Z. Liu, B. Tweedie, arXiv:1503.05923 [hep-ph], 2015.
- [57] V. Khachatryan, et al., CMS Collaboration, Phys. Rev. D 91 (2015) 012007, arXiv:1411.6530 [hep-ex];  
CMS Collaboration, CMS-PAS-EXO-12-038, 2013.
- [58] Search for long-lived, heavy particles in final states with a muon and a multi-track displaced vertex in proton–proton collisions at  $\sqrt{s} = 8$  TeV with the ATLAS detector, Tech. Rep. ATLAS-CONF-2013-092, 2013.
- [59] G. Aad, et al., ATLAS Collaboration, Phys. Lett. B 719 (2013) 280, arXiv:1210.7451 [hep-ex];  
G. Aad, et al., ATLAS Collaboration, Phys. Lett. B 707 (2012) 478, arXiv:1109.2242 [hep-ex].
- [60] G. Corcella, I. Knowles, G. Marchesini, S. Moretti, K. Odagiri, et al., J. High Energy Phys. 0101 (2001) 010, arXiv:hep-ph/0011363;  
G. Corcella, I. Knowles, G. Marchesini, S. Moretti, K. Odagiri, et al., arXiv:hep-ph/0210213, 2002.
- [61] E. Richter-Was, arXiv:hep-ph/0207355, 2002.
- [62] G.R. Farrar, P. Fayet, Phys. Lett. B 76 (1978) 575.
- [63] N. Nagata, H. Otono, S. Shirai, arXiv:1506.08206 [hep-ph].